DOI 10.1016/j.fuel.2020.118041

Study of the parameters of zeolites synthesis from coal fly ash in order to optimize their CO_2 adsorption

G. Verrecchia[a], L. Cafiero[a], B. de Caprariis[b], A. Dell'Era[c], I. Pettiti[d], R. Tuffi[a,*], M. Scarsella[b]

[a] *Department for Sustainability, ENEA – Casaccia Research Center, Via Anguillarese 301, S. Maria di Galeria, Rome, Italy.*

[b] *Department of Chemical Engineering, Sapienza University of Rome, Via Eudossiana 18, 00184, Rome, Italy.*

[c] *Department of Basic and Applied Sciences for Engineering, Sapienza University of Rome, Via Scarpa 16, 00161 Rome - Italy.*

[d] *Department of Chemistry, Sapienza University of Rome, P.le Aldo Moro 5, 00185, Rome, Italy*

[*] Corresponding author

E-mail address: riccardo.tuffi@enea.it

Abstract

The coal fly ash (CFA) from a coal gasification plant was used as raw materials for X zeolites synthesis by fusion and hydrothermal method and the ability of CFA-derived zeolites to adsorb CO_2 was studied. After characterization of CFA, factors affecting the synthesis of different zeolites from this CFA, i.e., NaOH/CFA weight ratio, crystallization temperature and crystallization time were investigated. X-ray powder diffraction showed that only the experimental conditions corresponding to 1.2 NaOH/CFA, 7 h and 90°C have led to a mixture composed by NaX and amorphous compounds without the formation of other crystalline structures. This product has a specific surface area of 498±4 m^2/g and exhibits a CO_2 adsorption capacity of 2.18 molCO_2/kg, corresponding to

57% of commercial 13X. Results showed that this feature is directly related to this specific crystalline product and not to other zeolitic forms or to amorphous phases. The design of experiment, named central composite full factorial, was accounted to optimize these synthesis parameters in order to maximize the CO_2 adsorption capacity of the CFA-derived zeolites. Thermogravimetry experiments showed that the experimental setting corresponding to 1.4 NaOH/CFA, 80°C and 7 h has led to a material with an adsorption capacity of 3.3 $molCO_2/kg$, the 86% of commercial 13X. Furthermore, results highlighted that all the examined synthesis parameter are significant for the purpose of improving CO_2 adsorption capacity of CFA-derived zeolites but too high values entail the production of more stable and useless (for this purpose) zeolites.

Keywords: coal fly ash, zeolite, fusion and hydrothermal treatment, design of experiment, carbon dioxide adsorption.

1. Introduction

Due to its abundancy and affordability in a large number of regions, coal fuels the largest share of worldwide electricity production. In 2018, world coal production was 8.0 billion tons, more than 70 wt% of which were used for power generation [1]. In the coal combustion and gasification process, large quantities of coal fly ash (CFA) are produced as by-product. Efficient disposal of CFA is a worldwide issue because of the huge amount produced and its harmful effects on the environment, caused by the pollution of air, water, and land [2]. To avoid the practice of CFA disposal in the sea or landfills, there is an increasing interest in material recovery from CFA.

CFA is an aggregate of spherical shape particles and primarily contains amorphous silica and alumina , in addition, minor crystal components such as, quartz, mullite, hematite and magnetite are present [3]. Due to its chemical composition, which is variable for different coal origins [2], CFA can be virtually used to produce new materials reducing the use of natural resources. Nowadays, the main use regards the manufacture of construction materials either as blended cements or geopolymers [4,5]. Other applications include catalysis [6], wastewater purification [7], gas adsorption [8], soil amendment [9], recovery of precious metals [10].

Many of these applications pass through the conversion of CFA into zeolites, exploiting the high CFA content of SiO_2 and Al_2O_3. Zeolites represent a large group of aluminosilicate minerals of tectosilicate type: a three dimensional framework of interconnected tetrahedrons, mainly comprising aluminum, silicon and oxygen atoms [11]. The peculiar chemical and structural properties of the different zeolites make them suitable for many technological applications [12].

Furthermore, controlled quantities of iron oxide, both present in CFA or expressly added let to obtain magnetic zeolites, easy to recover in water pollutants removal processes [13-15].

Many different zeolites, natural, synthetic and functionalized, are used for separation of CO_2 from gas streams [16]. Among others, X-type zeolites are the most widely reported physical adsorbents for CO_2 capture [17]. CO_2 capture and separation from flue gases have been considered as a key opportunity to reduce the greenhouse gases emissions from power plants [18]. On the other hand, a syngas or a biogas purified from CO_2 decreases its volume and, consequently, can be moved and stored reducing the operating costs. Furthermore, the combustion of a free CO_2 fuel gas (CO_2 has a null heating value) increases the energy produced per gas volume unit.

Many methods have been investigated for the synthesis of zeolites from CFA, depending on the chemical composition of the starting material and the type of zeolite to be produced [19]. According to the literature, these conversion techniques consist in: hydrothermal treatment [20], fusion followed by hydrothermal treatment [21], molten-salt treatment [22], microwave-assisted technique [23] ultrasound technique [24] or their combinations [25,26]. However, the fusion/hydrothermal methods are preferable as usually they involve a minor operational complexity. Furthermore, the other methods are more energy-intensive and have little potential for up-scale production [27].

The synthesis of zeolites from CFA through fusion/hydrothermal method is a complex phenomenon due to the multiplicity of involved variables. The main goal of this work is to study how some of these synthesis parameters such as NaOH/CFA weight ratio, crystallization time and crystallization temperature, can influence the nature of the produced zeolites and their ability to capture CO_2. Data in the literature confirm that CO_2 is effectively adsorbed on different CFA-derived zeolites but all the studies have focused on the characterization of the synthetized sorbent and on the investigation of the mechanism of the adsorption or the influence of different operation conditions on the adsorption of CO_2 on CFA-derived zeolite [17,29-34].

In particular, the CFA object of this study was characterized and deprivated by combustion of the residual carbon, without any further pre-treatment underwent the fusion followed by hydrothermal treatment in order to produce CFA-derived zeolites. Initially, macro variation of two out of three parameters (NaOH/CFA weight ratio and crystallization temperature) were carried out to reveal what combination leads to the desired zeolite formation. Then, the design of experiment (DOE) strategy, in particular the central composite full factorial design, has allowed to define the relationship between the moles of adsorbed CO_2 per kilogram of product and the three parameters (i.e. three independent variables) associated to the synthesis conditions. DOE is a collection of mathematical and statistical techniques useful to plan a set of experimental tests improving, developing and optimizing different variables simultaneously [35]. The DOE strategy was used by several authors in order to correlate different synthesis parameters with a particular property of the CFA-derived zeolite [3,36] but never with its CO_2 adsorption capacity. According to our knowledge, this study represents the first attempt to understand the correlation between the above mentioned synthesis parameters and the CO_2 adsorption capacity of a CFA-derived zeolite.

2. Experimental

2.1. Zeolite synthesis

DOI 10.1016/j.fuel.2020.118041

The raw CFA was collected from a coal gasification plant in Kolkata (India). After combustion at 550 °C in static air to remove unburnt carbon, CFA underwent chemical and morphological characterization followed by the fusion and hydrothermal treatment in order to produce CFA-derived zeolites. A first set of experiments was carried out varying extensively two parameters (NaOH/CFA ratio and crystallization temperature) in order to understand how these variables can affect the nature of the produced zeolite. Table 1 shows the six Test Runs (TRs) where the crystallization time was fixed at 7 hours. The parameters values for this first set of experiments were selected in the range of those reported by the published literature [11]. In particular, CFA and NaOH pellets (VWR Chemicals) were milled together with an exact ratio (1:1.2 or 1:1.8) and heated at 500 °C for 1 h. The fused mixture was then cooled to room temperature, milled again and added to distilled water with the weight ratio 10:1 (water/fused mixture). The resulting intermediate product followed the same steps of a classical hydrothermal treatment: after mechanical mixing at room temperature for 16 hours, it was hydrothermally treated for 7 hours at 90, 120 or 180 °C in a 125 ml non-stirred pressure vessel (Parr Instruments). The solid product obtained from each synthesis was filtered, washed with distilled water until pH 7, and dried overnight at 105 °C. Finally, the powder was milled again to remove the clumps. The product obtained from each TR was defined Product Run (PR).

Table 1

Variation of experimental parameters (NaOH/CFA weight ratio and crystallization temperature) in the first set of zeolite syntheses.

TR	NaOH/CFA weight ratio	Crystallization Temperature (°C)
1	1.2	90
2	1.2	120

DOI 10.1016/j.fuel.2020.118041

3	1.2	180
4	1.8	90
5	1.8	120
6	1.8	180

Subsequently, the synthesis optimization was carried out by Design Expert software (Stat-Ease, free trial). The effect of three variables (NaOH/CFA weight ratio, crystallization temperature and crystallization time) on CO_2 adsorption (moles of adsorbed CO_2 per kilogram of PR) was examined. The three variable of this second set of experimental tests were chosen following a central composite full factorial DOE where the levels of axial points in coded variables are determined by the Equation:

$$\alpha = \pm 2^{k/4} \tag{1}$$

Being k = 3 (the three independent chosen variables), α is ± 1.68. This design consists of three TR classes:

1. Eight TRs related to a 2^3 full factorial DOE, assuming two levels for each of the three independent variables;
2. one central TR performed for median values of the three independent variables;
3. six axial TRs carried out under identical conditions to the central test run except for a variable that will assume a higher or lower value than the levels established in 1.

The variation range of three variables start from the experimental conditions of TR1: NaOH/CFA weight ratio 1÷1.4, crystallization temperature 80÷100 °C and crystallization time 5÷7 h.

Table 2 summarizes the experimental conditions of the central composite full factorial DOE and the relative coded variables while Figure 1 is the representation of this kind of DOE.

Table 2

Experimental parameters (NaOH/CFA weight ratio, crystallization temperature and crystallization time) of the second set of zeolite syntheses and relative coded variables of the central composite full factorial DOE.

TR	NaOH/CFA weight ratio	Crystallization Temperature (°C)	Crystallization Time (h)	Coded variables*
7	1	80	5	-1; -1; -1
8	1	80	7	-1; -1; +1
9	1	100	5	-1; +1; -1
10	1	100	7	-1; +1; +1
11	1.4	80	5	+1; -1; -1
12	1.4	80	7	+1; -1; +1
13	1.4	100	5	+1; +1; -1
14	1.4	100	7	+1; +1; +1
15	1.2	90	6	0; 0; 0
16	1.53	90	6	+1.68; 0; 0
17	0.87	90	6	-1.68; 0; 0
18	1.2	107	6	0; +1.68; 0
19	1.2	73	6	0; -1.68; 0;
20	1.2	90	7.7	0; 0; +1.68
21	1.2	90	4.3	0; 0; -1.68

* The order of the coded variables is: NaOH/CFA weight ratio, crystallization temperature and crystallization time.

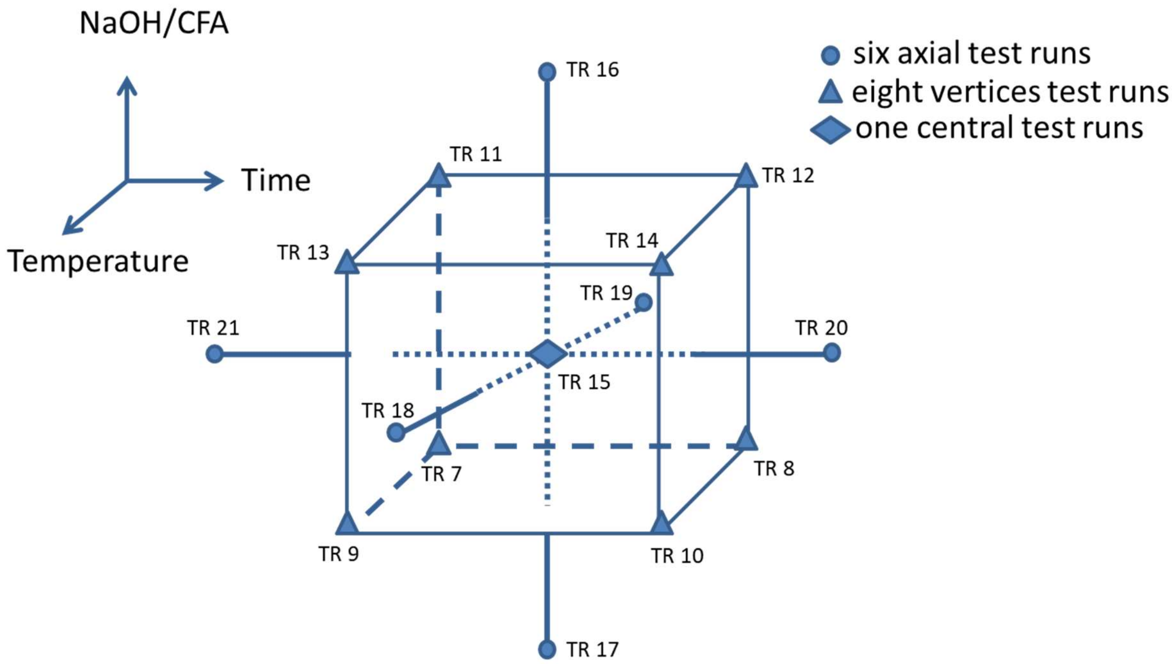

Fig 1. Representation of the central composite full factorial DOE with the fifteen TRs.

The synthesis of central TR15 was repeated six times as established by the central composite full factorial DOE.

2.2. Characterization of CFA and zeolites

CFA, the product of TR1 and a commercial zeolite 13X (Alfa Aesar) were chemically and physically characterized using different techniques. Field emission scanning electron microscopy (FESEM) performed by a high-resolution microscope (Auriga-Zeiss) helped to investigate the microstructure of raw CFA and zeolites. The initial chemical compositions of CFA was determined using FESEM/EDXS, and the percentage of oxides were calculated. The specific surface area was measured by nitrogen adsorption at the liquid nitrogen temperature (-196 °C) on powder samples pretreated at 350 °C under vacuum for 4 h, using a Micromeritics 3Flex 3500 analyzer. Brunauer-Emmett-Teller (BET) specific surface area was calculated in the range 0.005-0.1 P/P^0. The crystallinity of the samples was examined by X-ray diffraction (XRD) with a Philips PW 1830

GENERATOR diffractometer (CuKα radiation as a source of X-rays in the range 10°–80°). XRD was also used for the analysis of the PR 2÷6 and of collected little portions of the products of the steps adopted to produce TR1 in order to understand the nature of each single synthesis step.

2.3. CO_2 adsorption study

The CO_2 adsorption performance of CFA, commercial 13X, TR1÷6 and TR7÷21, determined by the central composite full factorial DOE, was evaluated by using a SETARAM 92-16.18 TGA. About 10 mg of the sample was placed into170 μL alumina pan. The sample was first heated from room temperature to 500 °C at a rate of 15 °C/min under pure Argon with a flow rate of 30 ml/min to remove the CO_2 and moisture adsorbed from the environment. Then, the sample was cooled down to 25 °C and kept at this temperature for 20 minutes. The CO_2 adsorption started opening the valve and flowing CO_2 with 35 ml/min flow rate for 30 minutes. The adsorption temperature was held at 25 °C to perform an isothermal experiment. The CO_2 adsorption capacity of the samples was calculated according to the mass change during the isothermal adsorption and reported as CO_2 moles adsorbed per PR kg.

For the samples PR1 and commercial 13X further TGA analyses were carried out: CO_2 sorption at ~~other~~ different temperatures (50, 100, 200, 300, 400 °C) after activation at 500 °C and CO_2 sorption at 25 °C after activation at different temperature (no activation, 160, 300, 400 °C) were conducted in order to study the effect of adsorption and activation temperature on the CO_2 adsorption capacity.

Subsequently, the results of TR7÷21 were processed by Design Expert software for statistical analysis and the final equation of the adsorption capacity as a function of the three independent variables, NaOH/CFA weight ratio, crystallization temperature and crystallization time was extracted. The significance level was set at 0.05.

3. Results and Discussion

3.1. Characterization of CFA

The XRD spectrum of raw CFA is shown in Figure 2, with reference materials taken from the Powder Diffraction File database. The XRD pattern highlights the presence of the mullite and quartz crystalline phases plus an undefined amount of amorphous phase. The mullite molecular formula is $Al_{4+2x}Si_{2-2x}O_{10-x}$ with $0.17 \leq x \leq 0.59$ [37]. In this case x is equal to 0.25 corresponding to $3Al_2O_3\ 2SiO_2$ in terms of alumina and silica and a silica-alumina molar ratio (SAR) of 0.7. In order to calculate the SAR of the whole CFA it is necessary to know the total amount of silica and alumina comprehensive of quartz and amorphous silica and alumina. For this purpose, a semi-quantitative elemental analysis was carried out by FESEM/EDXS and Table 2 reports the results in terms of weight percentage of oxides. The resulting composition is typical of CFA collected from eastern part of India [21]. The silica alumina weight ratio of 1.8 corresponding to a SAR of 3.1 is an indication of the possible synthesis of zeolite X from this CFA [11]. Actually, the formation of a particular zeolite also depends on the SAR of the raw material [11].

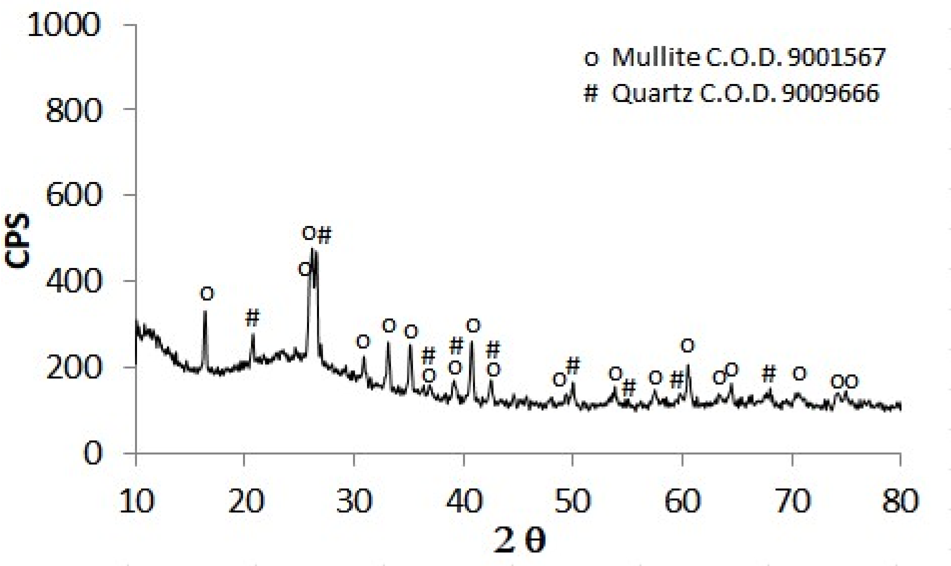

Fig 2. XRD spectrum of CFA.

Table 3. Chemical analysis of CFA.

Metal Oxide	Amount (wt%)
SiO_2	55.4
Al_2O_3	30.3
Fe_2O_3	3.5
TiO_2	3.3
CaO	3.1
MgO	0.2
K_2O	2.8
Na_2O	0.9
BaO	0.4
SiO_2/Al_2O_3	1.8

Figure 3 depicts the SEM images of the CFA. The particles have a regular spherical shape, but some spheres are not uniform and they are covered with smaller particles and irregular deposits (Figure 3a). The surface morphology highlights a porous (Figure 3b) or a compact (Figure 3c) structure as well. In any case the particles diameter is about in the range 100-200 μm. The smooth and spherical surface was mainly due to the amorphous glass phase that covers the particles. The physical characteristic of CFA depends on the particle size of feed coal, type of combustion, and the particulate control device [36].

DOI 10.1016/j.fuel.2020.118041

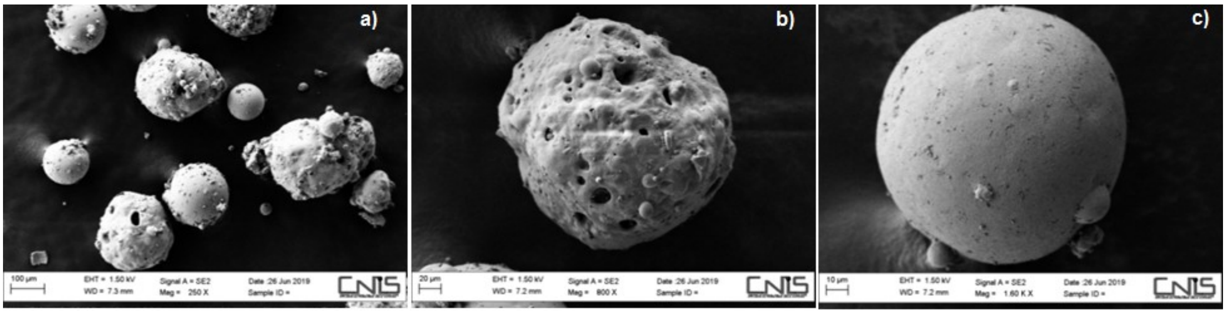

Fig 3. SEM images of CFA. From left to right, increasing magnification.

BET analysis has shown that CFA is mainly a macro-porous material with specific area 0.8±0.1 m^2/g. The total pore volume is very small and equal to 0.00059 cm^3/g while the pore diameter is distributed in the range 60÷1000 Å, with a maximum at about 432 Å.

Finally, these physico-chemical characteristics suggest that CFA is not a proper material for CO_2 capture as confirmed by null adsorption capacity during TGA experiment.

3.2. Experimental conditions: effect on NaX zeolite synthesis

Figure 4 shows the XRD spectra of the samples collected after each synthesis step of TR1. Combustion is necessary to remove the unburnt carbon but it does not modify the crystalline nature of CFA (Figure 4a): indeed, the crystalline phases mullite and quartz are still present. The fusion with NaOH at 500 °C converts alumina and/or silica compounds in sodium aluminate and sodium silicate salts soluble in water (Figure 4b). After 16 h mixing in water, a sample of the suspended solid is dried overnight at 105 °C and the XRD pattern (Figure 4c) shows its completely amorphous nature. This slurry composed by the amorphous suspended solid and the soluble salts is the precursor in an alkaline solution of nucleation reaction and growth of the zeolite crystals [11]. The synthesis intermediates of fusion with 1.8 NaOH/CFA weight ratio are very similar to those of fusion with 1.2 NaOH/CFA shown in Figure 4 for TR1. In fact, the XRD pattern of sodium

DOI 10.1016/j.fuel.2020.118041

aluminosilicate and sodium silicate is the same except for the height peaks ratio (Figure S1) and so the amorphous nature of suspended solid after mixing in water.

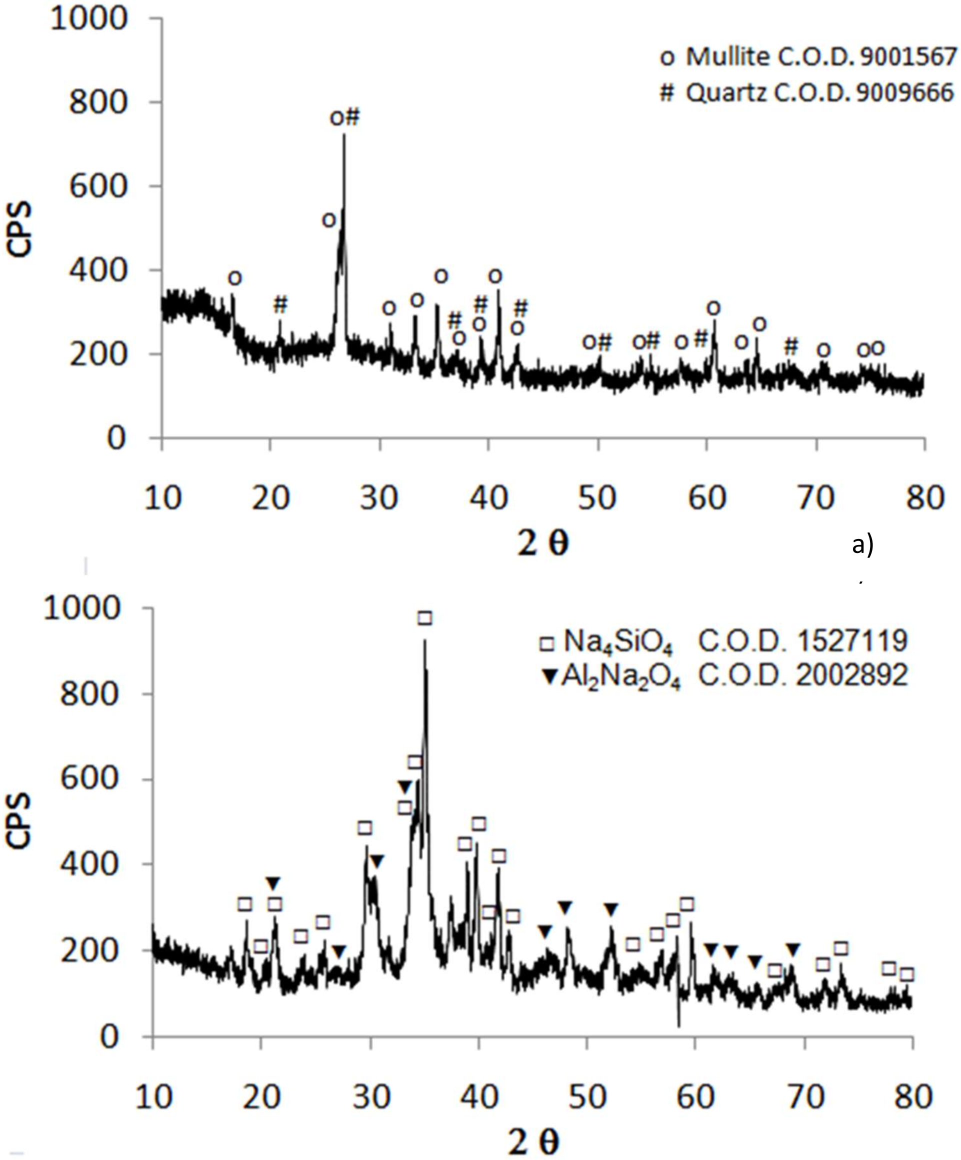

DOI 10.1016/j.fuel.2020.118041

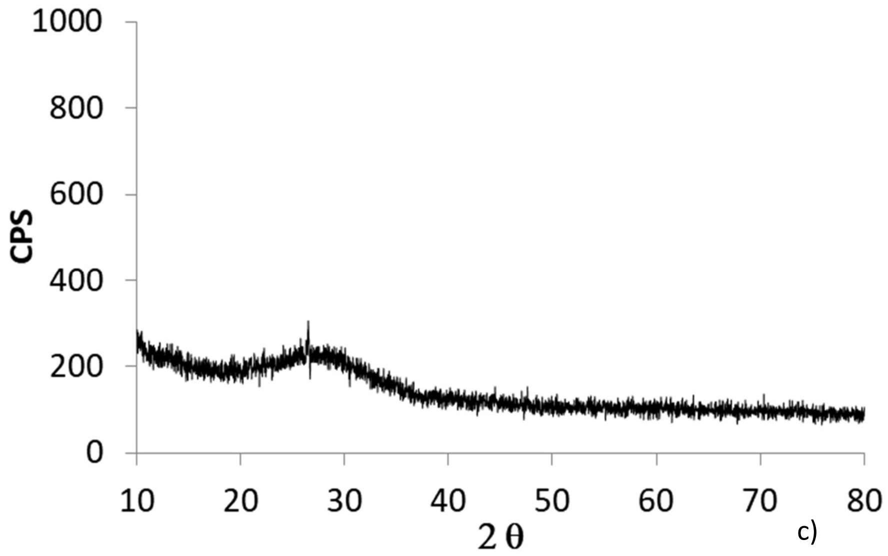

Fig4. XRD spectra of CFA after combustion (a), CFA after fusion with NaOH (TR1) (b), slurry (TR1) (c).

Nevertheless, the final products will be different because their nature and crystallinity are a function of the alkalinity of the reaction mixture as well as of the crystallization temperature [21]. In Figure 5 the XRD patterns of PR 1÷6 are reported. Comparing the obtained XRD patterns with that of commercial 13X (Figure S2), it is evident that only the experimental conditions of TR1 have uniquely led to the formation of NaX while the other TRs have given different types of zeolites. Higher NaOH/CFA weight ratios and crystallization temperatures have favored the formation of more stable zeolites: sodalite and/or cancrinite but also zeolite A in the case of PR4, obtained at the lower tested temperature. Zeolite X has a large pore size (7.3 Å) and a high cation-exchange capacity (CEC, 5 meq g^{-1}), which make this zeolite an interesting molecular sieve and a high-cation exchange material [12]. Zeolite X can be used to selectively adsorb CO_2 and water from gas streams and is used in the pre-purification of air for industrial air separation [3]. On the contrary, the small pore diameter of sodalite (2.3 Å) and the low CEC (0.3) [11] accounts for its limited potential application for both molecular sieving and ion exchange. Cancrinite is reported to be more thermodynamically stable than sodalite [38] although they show a similar pore diameter [39]. To conclude, Zeolite X is a metastable phase corresponding to a less condensed structure.

DOI 10.1016/j.fuel.2020.118041

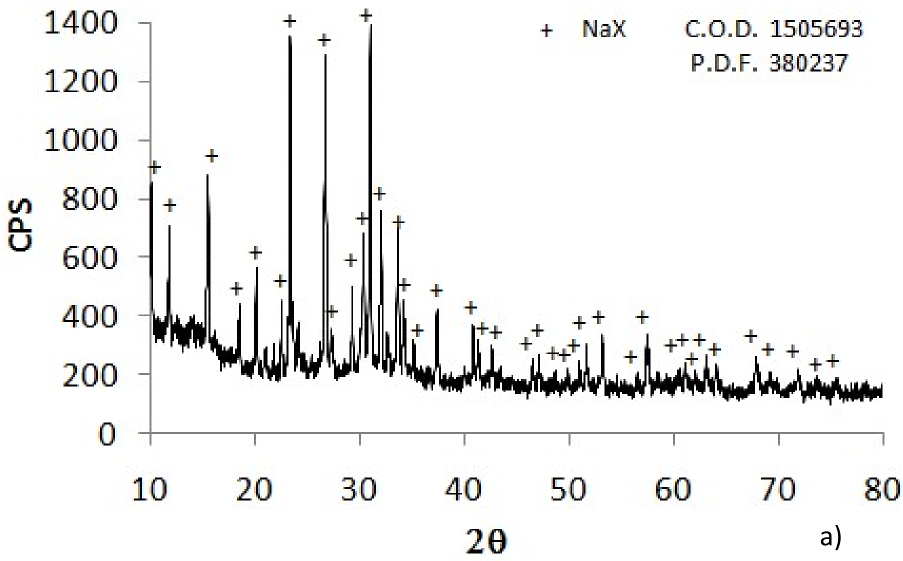

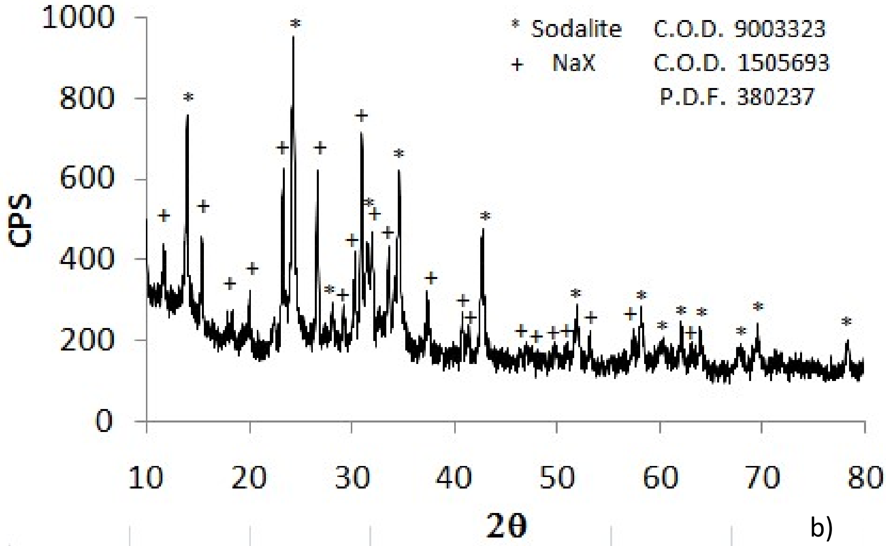

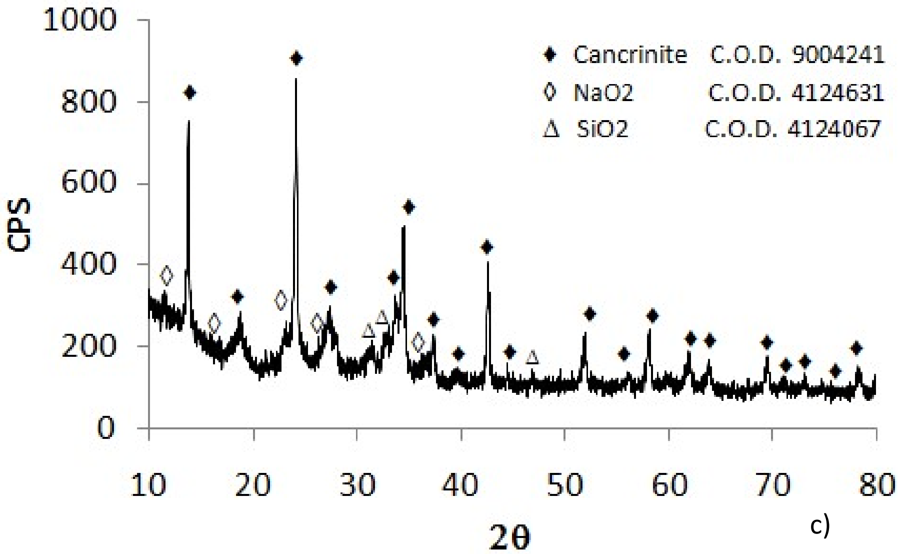

DOI 10.1016/j.fuel.2020.118041

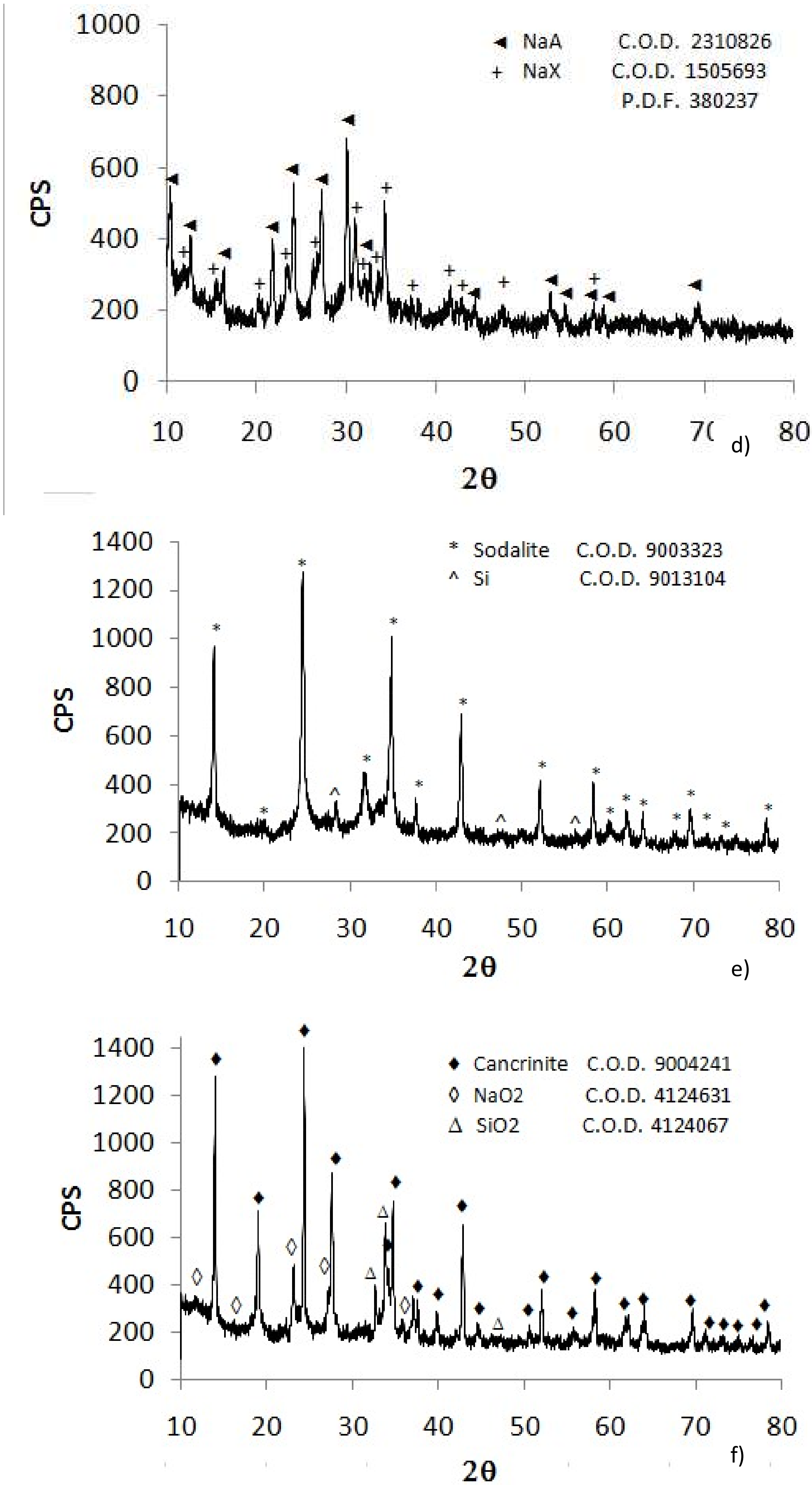

272 **Fig 5.** XRD spectra of PR1 (a), PR2(b), PR3 (c), PR4 (d), PR5 (e), PR6 (f).

More “energetic” conditions as well as longer synthesis time can increase the crystallinity, and consequently the zeolite quality, but also can lead to different types of zeolites, more dense and stable. As an example, Molina and Poole [40] showed that increasing NaOH/CFA weight ratio leads to an increase in the crystallinity and purity of the formed zeolitic product. Differently, the present work shows that, if TRs with the same crystallization temperatures are compared, the same evidence was found for TR3-TR6 couple, where the higher XRD peaks of PR6 reveal a greater production of cancrinite. On the contrary, for the couples TR1-TR4 and TR2-TR5, the higher NaOH/CFA weight ratios lead to the formation of more stable zeolites. Also Liu et al. [31] found that higher NaOH/CFA weight ratio promoted the formation of zeolite A to detriment of zeolite X from the same CFA source.

3.3. CO_2 adsorption

The CO_2 adsorption capacity of these six materials and commercial 13X was evaluated. Figure S3, as an example, shows the adsorption curves at 25 °C during the TGA experiments of PR1 and commercial 13X. The CO_2 adsorption kinetic was fast for both of them and with practical CO_2 adsorption equilibrium achieved with in few minutes.

TGA experiments revealed that only PRs in which NaX was present, showed a CO_2 adsorption capacity: the CO_2 adsorbed by PR1, PR2 and PR4 are 2.18, 1.81 and 0.6 $molCO_2/kgPR$, respectively while PR3, PR5 and PR6 does not adsorb CO_2 at all. Sodalite and cancrinite are poor adsorbent because of their small pore diameters. Also the amorphous slurry and the CFA fused with soda (the reaction intermediates of TR1) have been undergone TGA CO_2 adsorption experiment and neither showed an adsorption capacity. Therefore, this property is directly correlated with the crystalline form of NaX zeolite. Commercial 13X resulted to have a CO_2 adsorption capacity of

3.84 molCO_2/kgzeo and, then the adsorption capacity of PRs with NaX (at least in the case of PR1) makes this material a prospective low cost material for the CO_2 capture.

In Table 4 an explicative summary of the performance of some CFA-derived material is provided. Taking into account the different operating conditions, PR1 showed an adsorption capacity consistent with the values reported in literature.

Table 4. Literature review on CO_2 adsorption capacity of CFA-derived zeolites**.**

CFA-derived zeolites	**Synthesis conditions**			**CO_2 adsorption**				**References**
	NaOH/CFA weight ratio	**Crystallization Temperature (°C)**	**Crystallization Time (h)**	**Experimental Apparatus**	**Pressure (bar)**	**Temperature (°C)**	**Uptake (mol/kg)**	
NaX	0.45	95	6-16	TGA	1	25	5.11	[18]
Cancrinite	1.2	140	5	Calorimeter	--	30	0.13	[29]
NaP1	0.96*	100	24	TGA	0.1	25	0.77	[30]
NaA	1.2	100	12	TGA	0.1	25	1.18	[30]
NaA	2	80	24	Volumetric	1	30	3.5	[31]
NaA+NaX	1.2	80	24	Volumetric	1	30	~ 4.4	[31]
NaA	--**	100	5	Fixed bed	0.05	20	0.56	[32]
4A-X blend	0.24***	80	10	Glass reactor	0.3	-78	1.68	[33]
NaX	2	90	2	TGA	0.5	22	1.36	[34]

*160 mL of NaOH solution 3 M with 20 g CFA
**1.23/1.2/1 $NaAlO_2$/Na_2CO_3/CFA fused at 800 °C
***the silica extract obtained after stirring at 90 °C for 6 h was mixed with a waste water from an Al-anodising plant containing 57.6 g/l Al and 14.9 g/l NaOH

DOI 10.1016/j.fuel.2020.118041

Also the effect of adsorption and activation temperature on CO_2 adsorption capacity were studied and the relative curves are reported in Figure 6.

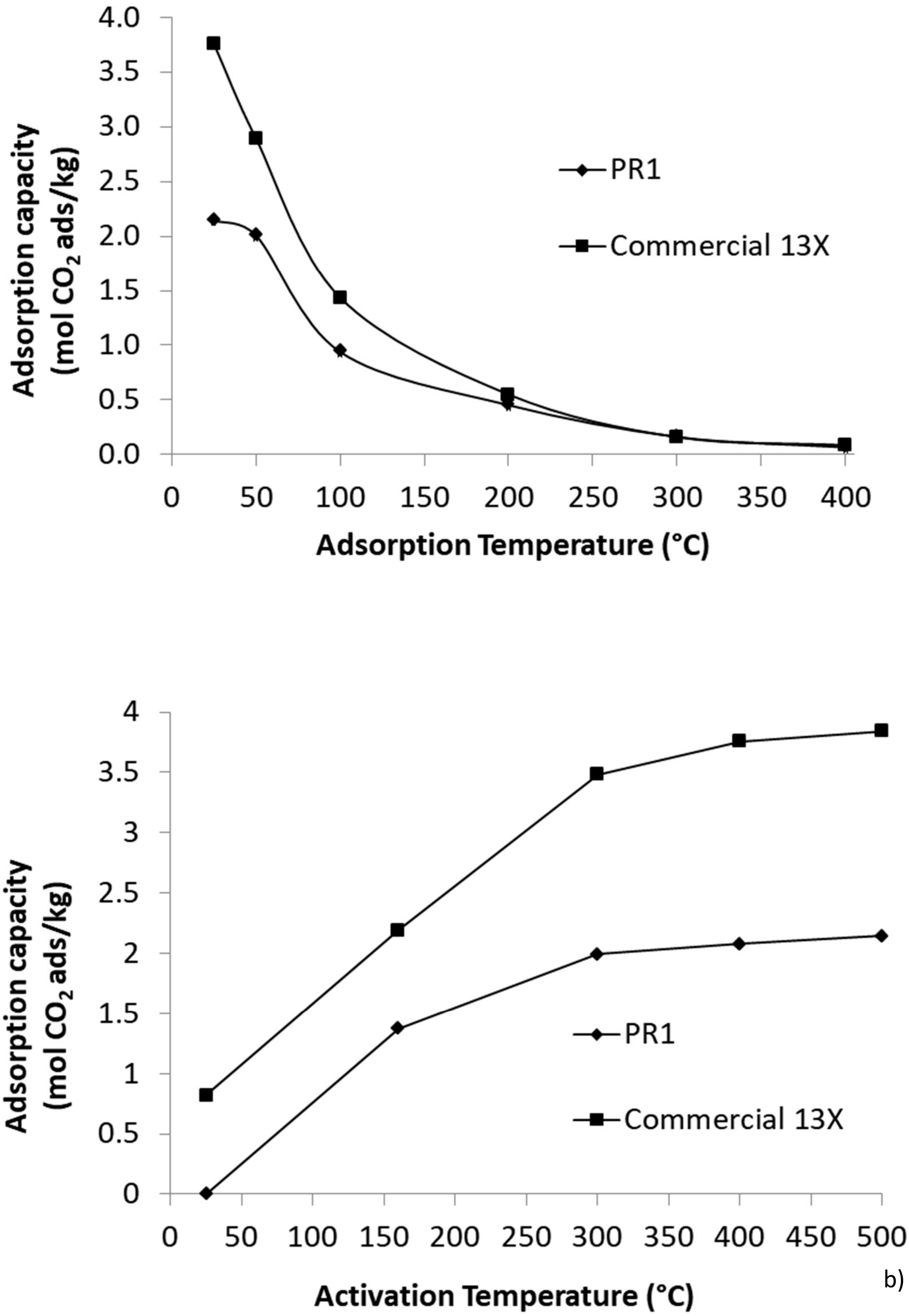

Fig 6. Adsorption temperature (a) and activation temperature (b) dependence of adsorption capacity for PR1 and Commercial 13X.

DOI 10.1016/j.fuel.2020.118041

Temperature is a crucial factor for the CO_2 adsorption capacity performance of CFA-derived zeolites as well as pure zeolites. In Figure 6a it is evident that an increasing temperature leads to a steep fall of both PR1 and commercial 13X adsorption capacity. After 200 °C the two curves tend to overlap and the amount of adsorbed CO_2 becomes not significant. Therefore, the removal of CO_2 from flue gases on zeolites should be carried out at temperature as low as possible. On the other hand, before using their sorption properties, zeolites must ~~have~~ undergone a thermal activation process in order to clean the channel network from water (mainly) and other gaseous molecules [30]. The CO_2 adsorption capacity of PR1 and commercial 13X at 25 °C after activation processes conducted at temperatures ≤ 500 °C (in dynamic heating conditions) is shown in Figure 6b. As it can be observed, also the activation temperature significantly influenced CO_2 adsorption capacity of zeolite NaX: PR1 progresses from a null adsorption after no activation to 1.37 $molCO_2/kgPR$ after activation at 160 °C and 2.14 $molCO_2/kgPR$ after activation at 500 °C. Low activation temperatures cause an incomplete removal of water and other gases that block the access for CO_2 reduce the adsorption capacity of these materials in the same conditions of pressure and temperature. This evidence means that a high moisture content in flue gases makes zeolites unsuitable CO_2 sorbents because it is competitively adsorbed on the zeolite surface [16]. In these cases an upstream dehydration system must be considered [41]. Another solution can be the utilization of amines grafted or impregnated on zeolites or CFA-derived zeolites thanks to their high uptakes in moist flue gases with CO_2 at low partial pressures [42].

3.4. Characteristics of PR1

PR1 was undergone further characterization. Quantitative measure of the yield of the synthesized zeolite was made by using the summed heights of major peaks in the X-ray diffraction of PR1 and commercial 13X [11]:

DOI 10.1016/j.fuel.2020.118041

$$\% \text{ yield} = \frac{\sum peak\ heigh\quad of\ synthetized\ material}{\sum peak\ height\quad of\ standard\ material} \tag{2}$$

The percentage of crystallinity of PR1 corresponds to the NaX yield and resulted to be 60%, in accordance with yields reported in literature for CFA-derived zeolites [11,43,44]. Since no other crystal phases are present, about 40 wt% of PR1 is composed by amorphous materials. Mullite, quartz, silica and alumina are the major reactive phases during zeolite synthesis from CFA after alkali activation. The percentage of yield lower than 100% can depend on the unreacted alumino-silicates and the fraction of the other chemical species in CFA inert in this synthesis. Really, hematite and the other metal oxides do not affect the activation but their separation (e.g. with an acid treatment) prior to zeolite synthesis results in an increase in conversion efficiency [20].

Furthermore, specific surface area of PR1 was 498±4 m^2/g and the presence of a slight hysteresis in N_2 adsorption isotherm (Figure S4) shows that the sample is mainly microporous with a little portion of mesopores (41 m^2/g are due to its external surface area and mesopores and the pore size distribution is shown in Figure S5). The total pore volume of PR1 is 0.274 cm^3/g, 0.183 cm^3/g relative to micropores. Commercial 13X is substantially microporous with a surface area value equal to 865±7 m^2/g, of which 855 m^2/g are due to micropores. The residual surface area (10 m^2/g) is due to the external surface area of 13X and to very few mesopores present in a commercial zeolite (Figure S5). The total pore volume is 0.354 cm^3/g, 0.338 cm^3/g relative to micropores.

A correlation between CO_2 adsorption and surface area or pore volume in zeolites, particularly in 13X type, is not easy and it is widely debated in literature owing to the existence of different adsorbent-adsorbate interactions related to the porosity of the zeolitic complex system, to the presence of extra-framework cations and to the heterogeneity of adsorption centers [45]. Although this is far from the goal of the present work, an effort to relate CO_2 adsorption to the structural features of PR1 in a simple way, as suggested by Zhonglin et al. [45], could be made. In PR1 the effective adsorption surface area is 57.6% with respect to commercial 13X; it is mainly due to the

DOI 10.1016/j.fuel.2020.118041

presence of the crystalline zeolitic phase because the amorphous phase contribution is about 30 m^2/g, (after deduction of external surface area) ~~supposing that there are not zeolite crystals not detectable by XRD analysis in the amorphous phase~~. CO_2 adsorption in PR1 is 56.8% with respect to commercial 13X and the effective surface area is the simplest way to relate these data, but it could be not the only one. In fact, the ratio between micropore volumes of PR1 and commercial 13X is 0.541 and it could also be related to the amount of adsorbed CO_2 as suggested by Rehman and Park [46,47] for nitrogen-doped ultra-microporous carbons. The first hypothesis seems to be sustained by a previous work where the BET analysis of an amorphous material synthetized by CFA through a similar procedure showed a specific surface area of 31 m^2/g [6] and by similar crystallites dimension of PR1 and commercial 13X revealed by SEM analysis.

Indeed, the SEM images of PR1 and commercial 13X are compared in Figure 7 showing that the crystallites of PR1 sample have a cubic or octahedral morphology and not uniform size. Some particles are covered with smaller ones and irregular deposits evidencing a rough surface with not clearly distinguishable facets. Instead, the commercial 13X sample presents crystallites with octahedral habit and micrometric uniform size showing a smooth surface with distinguishable facets.

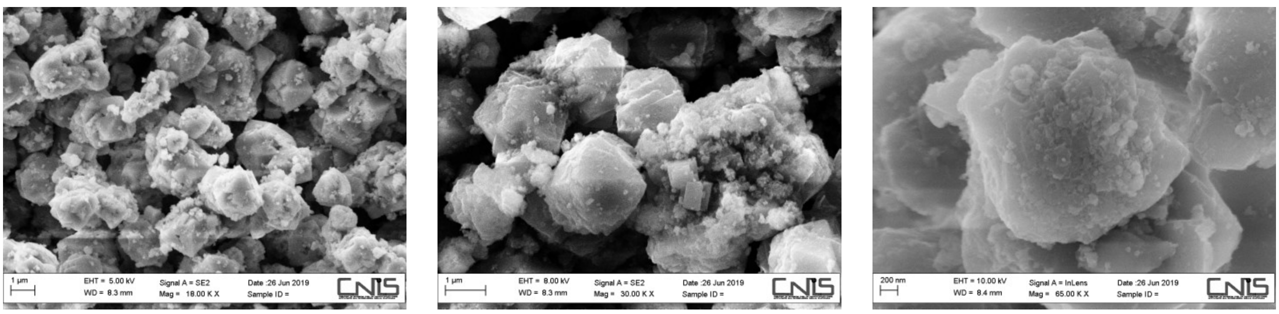

DOI 10.1016/j.fuel.2020.118041

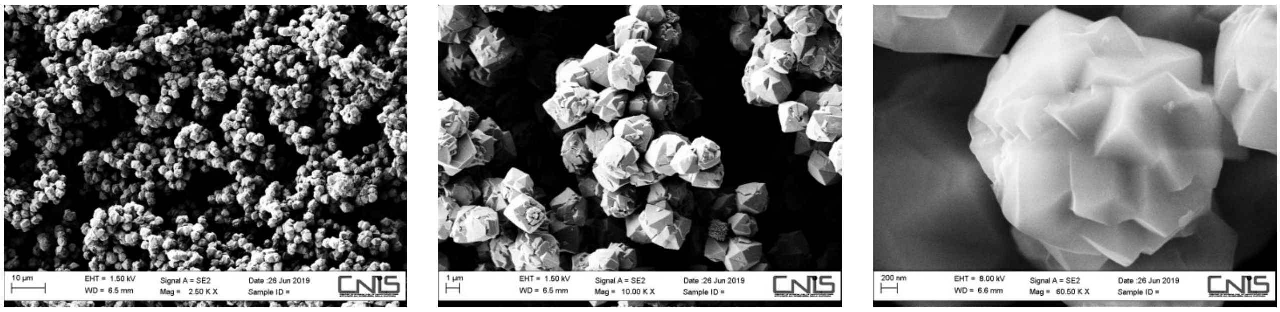

Fig 7. SEM images of PR1 (above) and commercial 13X (below). From left to right, increasing magnification.

3.3. Optimization of design parameters for NaX synthesis.

Since cancrinite or sodalite showed a null CO_2 adsorption capacity and there is no industrial or applicative interest in their synthesis, the second part of the present work focused on the optimization of synthesis parameters of NaX in terms of its ability to adsorb CO_2, starting from the experimental conditions of TR1. In Table 5 the results of TGA experiments on the central composite full factorial DOE syntheses were reported.

Table 5. CO_2 adsorbed by PRs in isothermal conditions at 25 °C following the central composite full factorial DOE.

PR	**Adsorption capacity (mol CO_2 ads/kg PR)**
7	0
8	0
9	0
10	0.633
11	2.815
12	3.307

13	1.398
14	1.298
15	2.391
15	2.522
15	2.468
15	2.476
15	2.412
15	2.44
16	2.91
17	0
18	0.72
19	1.711
20	1.784
21	1.147

The PR7, 8, 9 and 17 adsorbed a null amount of CO_2 and XRD analysis confirmed that they are mainly composed by an amorphous material. The system is not energetic enough to crystallize the aluminosilicate slurry in a zeolite. As an example, in Figure S5 it can be noted that PR7 XRD pattern has still the peaks related to quartz: the low ratio NaOH/CFA was not enough to completely fuse CFA. The other PRs have shown an adsorbent capacity in the range 0.6÷3.3 $molCO_2/kgPR$. PR12 ensured the best performance, reaching the 86% of 13X adsorption capacity. In order to be competitive with existing processes using aqueous solutions of amines, the CO_2 capacity of a solid sorbent must be in the range of 3-4 $molCO_2/kg$ [16]. The mean value and the low standard deviation of the six replicas of PR15 (2.45 ± 0.05 $molCO_2/kgPR$) have verified that the synthesis procedure is reliable. As for the fitness of proposed model, the actual versus predicted plots shown in Figure 8 while the results of analysis of variance (ANOVA) for the CO_2 adsorption capacity of selected factorial model are reported in Table 6.

Tab 6. Results of ANOVA for the adsorption capacity of factorial model.

Source	DF	Adj SS	Adj MS	F-Value	P-Value
Model	9	22.4317	2.4924	69.27	0.000
Linear	3	14.3041	4.7680	132.52	0.000
NaOH/CFA	1	12.5256	12.5256	348.13	0.000
Temperature	1	1.4563	1.4563	40.48	0.000
Time	1	0.3222	0.3222	8.95	0.014
Square	3	6.0607	2.0202	56.15	0.000
NaOH/CFA*NaOH/CFA	1	2.0837	2.0837	57.91	0.000
Temperature*Temperature	1	3.1150	3.1150	86.58	0.000
Time*Time	1	2.0417	2.0417	56.75	0.000
2-Way Interaction	3	2.0669	0.6890	19.15	0.000
NaOH/CFA*Temperature	1	2.0594	2.0594	57.24	0.000
NaOH/CFA*Time	1	0.0073	0.0073	0.20	0.663
Temperature*Time	1	0.0002	0.0002	0.01	0.941
Error	10	0.3598	0.0360		
Lack-of-Fit	5	0.3486	0.0697	31.14	0.001
Pure Error	5	0.0112	0.0022		
Total	19	22.7915			
Summary of quadratic model	S	R^2	Adj R^2	Pred R^2	
	0.1897	0.9842	0.9700	0.8703	

DF: degree of freedom; Adj SS: adjusted sum of squares; Adj MS: adjusted mean square.

DOI 10.1016/j.fuel.2020.118041

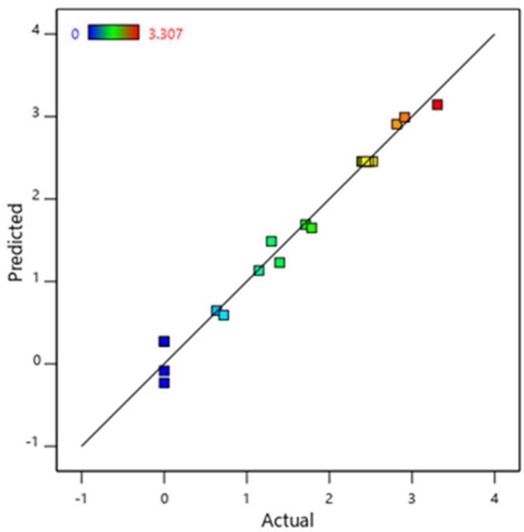

Fig 8. Actual vs. predicted plot of adsorption capacity (molCO_2/kgPR).

The plot clearly describes the closeness of actual and predicted values for CO_2 adsorption capacity. The calculated model satisfactorily correlates the TGA results of the CO_2 adsorption experiments. The most significant deviations from the model were due to the null values of some PRs that cause a not complete overlap between the adjusted and predicted R^2 value (0.97 and 0.87, respectively). Equation (2) represents the model of quadratic regression in coded variables:

$$\text{mol}CO_2/\text{kgPR} = 2.4558 + 0.9577(\text{NaOH/CFA}) - 0.3266(\text{Temperature}) + 0.1536(\text{Time}) - 0.3802(\text{NaOH/CFA})^2 - 0.4649(\text{Temperature})^2 - 0.3764(\text{Time})^2 - 0.5074(\text{NaOH/CFA*Temperature}) - 0.0301(\text{NaOH/CFA*Time}) + 0.0051(\text{Temperature*Time}) \quad (2)$$

From Equation (2), it can be stated that among the three studied parameters the NaOH/CFA weight ratio has the most significant effect on CO_2 adsorption capacity of the synthetized material. This is evident also observing Figure 9, where the plot (a) reaches the maximum CO_2 adsorption capacity. On the contrary, the least significant factors are the 2-Way Interactions (NaOH/CFA*Time) and (Temperature*Time). Furthermore, Figure 8 shows, as expected that increasing indefinitely the

DOI 10.1016/j.fuel.2020.118041

three parameters do not implicate a relative increase in the CO_2 adsorption capacity of the synthetized material. Instead, after reaching the maximum, CO_2 adsorption capacity decreases as a function of NaOH/CFA weight ratio, temperature or time. This behavior is understandable in the light of what observed in the *paragraph 3.2*: it is necessary to supply "energy" in order to fuse CFA and to crystallize the amorphous aluminosilicate slurry but too much energy will form highly stable zeolites not useful for the purpose of CO_2 capture.

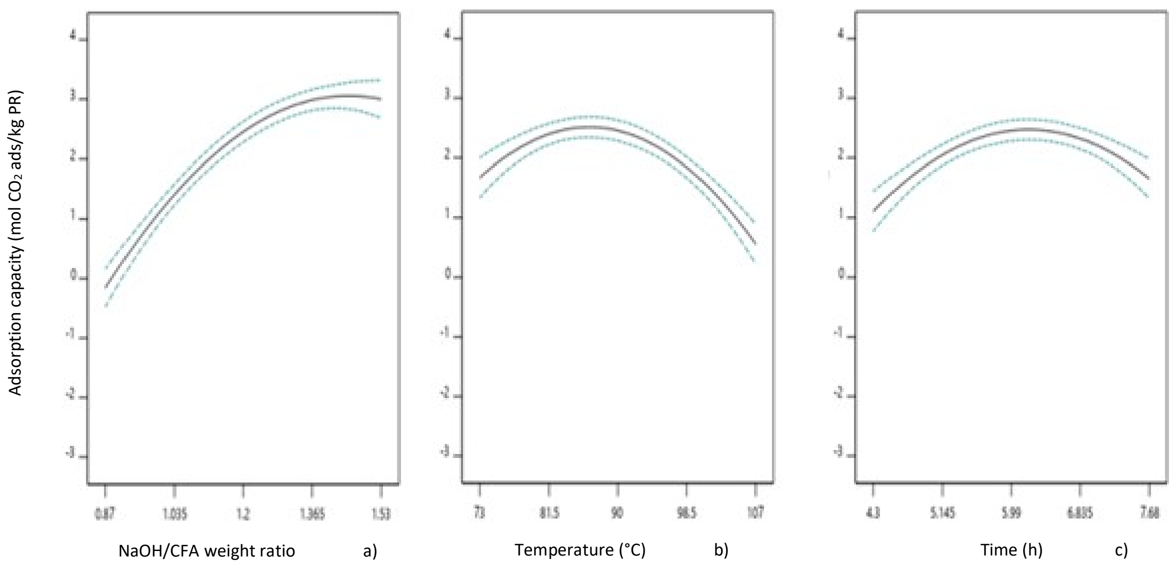

Fig 9. Different response of adsorption capacity ($molCO_2/kgPR$) to NaOH weight ratio (a), Temperature (b) and Time (c).

4. Conclusion

In this paper, the effect of three parameters (NaOH/CFA weight ratio, crystallization time and crystallization temperature) involved in the zeolite synthesis from CFA was investigated in order to obtain an effective material for carbon dioxide capture. In the first phase of the work the three synthesis parameters were set in order to produce a X-type zeolite from CFA by alkali fusion followed by hydrothermal treatment. The experimental conditions corresponding to NaOH/CFA

DOI 10.1016/j.fuel.2020.118041

weight ratio, crystallization time and crystallization temperature equal to 1.2, 7 h and 90 °C, respectively have led to a mixture composed by NaX, the unique present crystalline phase, and unreacted amorphous compounds. This material has been morphologically characterized and resulted to adsorb 2.18 molCO_2/kg, about 60% of CO_2 adsorption capacity of commercial 13X. The study continued with the optimization of synthesis procedure in order to improve the CO_2 adsorption capacity of the CFA-derived zeolites. The optimization of the synthesis procedure was carried out with the help of DOE strategy, in particular following the central composite full factorial design. Among the different TRs of this second synthesis set, the best conditions for the maximum CO_2 adsorption capacity were found as NaOH/CFA weight ratio of 1.4, the crystallization temperature of 80 °C and crystallization time of 7 h. The relative product showed a CO_2 adsorption capacity of 3.3 molCO_2/kg, reaching the 86% of 13X adsorption capacity. All the examined synthesis parameter are significant for the purpose of improving CO_2 adsorption capacity but their indefinite increase do not lead to better performances but only to more stable and useless zeolitic forms. Although these considerations may have a general value, it is important to highlight that the optimized conditions are closely related to the specific origin of CFA.

To conclude, this study gives a new and alternative approach for CFA recycling, proposing a method to manufacture a low cost X-type zeolite that in the future can be highly in demand for reversible capture processes of greenhouse gases. The research outlook will concern the study of the process of CO_2 adsorption onto CFA-derived zeolite in dynamic column in order to facilitate the up-scaling from laboratory to pilot installations.

Funding sources

This research did not receive any specific grant from funding agencies in the public, commercial, or not-for-profit sectors.

References

[1] BP Statistical Review of World Energy, 2019, 68^{th} Edition. Available at https://www.bp.com/content/dam/bp/business-sites/en/global/corporate/pdfs/energy-economics/statistical-review/bp-stats-review-2019-full-report.pdf.

[2] Wang S. Application of solid ash based catalysts in heterogeneous catalysis. Environ Sci Technol 2008; 42(19):7055–7063.

[3] Sivalingam S, Sen S. Optimization of synthesis parameters and characterization of coal fly ash derived microporous zeolite X. Appl Surf Sci 2018; 455: 903–910.

[4] González A, Navia R, Moreno N. Fly ashes from coal and petroleum coke combustion: current and innovative potential applications. Waste Manage Res 2009; 27(10): 976–987.

[5] Zhuang XY, Chen L, Komarneni S, Zhou CH, Tong DS, Yang HM, Yu WH, Wang H. Fly ash-based geopolymer: clean production, properties and applications. J Clean Prod 2016; 125: 253–267.

[6] Benedetti M, Cafiero LM, De Angelis D, Dell'Era A, Pasquali M, Stendardo S, Tuffi R, Vecchio Ciprioti S. Pyrolysis of WEEE plastics using catalysts produced from fly ash of coal gasification. Front Env Sci Eng 2017; 11: 11–21.

[7] Koshy N, Singh DN. Fly ash zeolite for water treatment applications. J Environ Chem Eng 2016; 4: 1460-1472.

[8] Wang SB, Wu HW. Environmental-benign utilization of fly ash as low-cost adsorbents. J Hazard Mater 2006; 136(3): 482–501.

[9] Yunusa IAM, Eamus D, DeSilva DL, Murray BR, Burchett MD, Skilbeck GC, Heidrich C. Fly-ash: An exploitable resource for management of australian agricultural soils. Fuel 2006; 85(16): 2337–2344.

[10] Torralvo FA, Fernández-Pereira C. Recovery of germanium from real fly ash leachates by ion-exchange extraction. Miner Eng 2011; 24: 35–41.

DOI 10.1016/j.fuel.2020.118041

[11] Jha B, Singh DN. Fly Ash Zeolites. Innovations, Applications, and Directions. 1st ed. Singapore: Springer; 2016.

[12] Querol X, Moreno N, Umaña JC, Alastuey A, Hernandez E, Lopez-Soler A, Plana F. Synthesis of zeolites from coal fly ash: an overview. Int J Coal Geol 2002; 50: 413–423.

[13] Oliveira LCA, Petkowicz DI, Smaniotto A, Pergher SBC. Magnetic zeolites: a new adsorbent for removal of metallic contaminants from water. Water Res 2004; 38: 3699–704.

[14] Supelano GI, Gómez Cuaspud JA, Moreno-Aldana LC, Ortiz C, Trujillo CA, Palacio CA, Parra Vargas CA, Mejía Gómez JA. Synthesis of magnetic zeolites from recycled fly ash for adsorption of methylene blue. Fuel 2020; 263: 116800.

[15] Yuan M, Xie T, Yan G, Chen Q, Wang L. Effective removal of Pb^{2+} from aqueous solutions by magnetically modified zeolite. Powder Technol 2018; 332: 234–241.

[16] Samanta A, Zhao A, Shimizu GKH, Sarkar P, Gupta R. Post-combustion CO_2 capture using solid sorbents: A review. Ind. Eng. Chem. Res. 2012; 51: 1438–1463.

[17] Lee SY, Park SJ. A review on solid adsorbents for carbon dioxide capture. J Ind Eng Chem 2015; 23: 1–13.

[18] Zhang Z, Xiao Y, Wang B, Sun Q, Liu H. Waste is a misplayed resource: synthesis of zeolites from fly ash for CO_2 capture. Enrgy Proced 2017; 114: 2537–2544.

[19] Wdowin M, Franus M, Panek R, Badura L, Franus W. The conversion technology of fly ash into zeolites. Clean Technol Envir 2014; 16:1217–1223.

[20] Mondragón F, Rincón F, Seirra L, Escobar J, Ramierez J, Fernández J. New perspectives for coal ash utilization: synthesis of zeolitic materials. Fuel 1990; 69: 263–266.

[21] Ojha K, Pradhan NC, Samanta AN. Zeolite from fly ash: synthesis and characterization. Bull Mater Sci 2004; 27(6): 555–564.

[22] Park M, Choi CL, Lim WT, Kim MC, Choi J, Heo NH. Molten-salt method for the synthesis of zeolitic materials II. Characterization of zeolitic materials, Micropor Mesopor Mat 2000; 37: 91–98.

[23] Tanaka H, Fujimoto S, Fujii A, Hino R, Kawazoe T. Microwave Assisted Two-Step Process for Rapid Synthesis of Na−A Zeolite from Coal Fly Ash. Ind Eng Chem Res 2008; 47(1): 226–230.

[24] Belviso C, Cavalcante F, Lettino A, Fiore S. Effects of ultrasonic treatment on zeolite synthesized from coal fly ash. Ultrason Sonochem 2011; 18: 661–668.

[25] Aldahri T, Behin J, Kazemian H, Rohani S. Effect of microwave irradiation on crystal growth of zeolitized coal fly ash with different solid/liquid ratios. Adv Powder Technol 2017; 28(11): 2865–2874.

[26] Bukhari SS, Rohani S, Kazemian H. Effect of ultrasound energy on the zeolitization of chemical extracts from fused coal fly ash. Ultrason Sonochem 2016; 28: 47–53.

[27] Li Xin Hong J, Maneerung T, NuoKoh S, Kawi S, Wang CH. Conversion of coal fly ash into zeolite materials: synthesis and characterizations, process design, and its cost-benefit analysis. Ind Eng Chem Res 2017; 56: 11565−11574.

[28] Beltrao-Nunes AP, Sennour R, Arus VA, Anoma S, Pires M, Bouazizi N, Roy R, Azzouz A. CO_2 capture by coal ash-derived zeolites- roles of the intrinsic basicity and hydrophilic character. J. Alloy Compd. 2019, 778: 866-877.

[29] Dindi A, Quang DV, MRM Abu-Zahra. CO_2 Adsorption Testing on Fly Ash Derived Cancrinite-type Zeolite and its Amine-Functionalized Derivatives. Environ. Prog. Sustain. 2019, 38 (1): 77-88.

[30] Majchrzak-Kuçeba I, Nowak W. A thermogravimetric study of the adsorption of CO_2 on zeolites synthesized from fly ash, Thermochim. Acta 2005, 437: 67–74.

[31] Liu L, Singh R, Xiao P, Webley PA,·Zhai Y. Zeolite synthesis from waste fly ash and its application in CO_2 capture from flue gas streams. Adsorpt. 2011; 17: 795–800.

[32] Lee CH, Park SW, Kim SS. Breakthrough analysis of carbon dioxide adsorption on zeolite synthesized from fly ash, Kor. J. Chem. Eng. 2014, 31: 179-187.

[33] Querol X, Moreno N, Umaña JC, Juan R, Hernàndez S, Fernandez-Pereira C, Ayora C, Janssen M, Garcìa -Martìnez J, Linares-Solano A, Cazorla-Amoros D. Application of zeolitic material synthesized from fly ash to the decontamination of waste water and flue gas, J. Chem. Technol. Biotechnol. 2002, 77: 292-298.

[34] Kalvachev Y, Zgureva D, Boycheva S, Barbov B. Synthesis of carbon dioxide adsorbents by zeolitization of fly ash. J. Therm. Anal. Calorim. 2016, 124: 101-106.

[35] Lazic ZR. Design of Experiments in Chemical Engineering. 1st ed. Weinheim: Wiley-VCH; 2004.

[36] Musyoka NM, Petrik LF, Balfour G, Ndungu P, Gitari WM, Hums E. Synthesis of zeolites from coal fly ash: application of a statistical experimental design. Res. Chem. Intermed. 2012; 38: 471–486.

[37] Cameron WE. Mullite: a substituted alumina. Am Mineral 1977; 62: 747–755.

[38] Barnes MC, Addai-Mensah J, Gerson AR. The mechanism of the sodalite-to-cancrinite phase transformation in synthetic spent Bayer liquor. Micropor Mesopor Mater 1999; 31: 287–302.

[39] Huertas-Miranda JA, Quinones-Fontalvo L, Martinez Inesta MM. Molecular simulation for the synthesis of Ni nanowires in zeolite cancrinite. NSTI-Nanotech 2009; 3: 280–283.

[40] Molina A, Poole C. A comparative study using two methods to produce zeolites from fly ash. Miner Eng 2004; 17: 167–173.

[41] Zgureva D. Carbon dioxide adsorption studies on fly ash zeolites. CCGP 2016, 8: 54-59.

[42] Panek R, Wdowin M, Franus W, Czarna D, Stevens LA, Deng H, Liu J, Sun C, Liu H, Snape CE. Fly ash-derived MCM-41 as a low-cost silica support for polyethyleneimine in post-combustion CO_2 capture. J. CO_2 Util. 2017, 22: 81-90.

[43] Rayalu S, Meshram SU, Hasan MZ. Highly crystalline faujasitic zeolites from fly ash. J Hazard Mater 2000; 77: 123–131.

DOI 10.1016/j.fuel.2020.118041

[44] Chareonpanich M, Namto T, Kongkachuichay P, Limtrakul J. Synthesis of ZSM-5 zeolite from lignite fly ash and rice husk ash. Fuel Process Technol 2004; 85: 1623–1634.

[45] Zhonglin Z, Xingyu C, Jinghong M, Ruifeng L. Adsorption of carbon dioxide on alkali-modified zeolite 13X adsorbents. Int J Greenh Gas Con 2007; 1: 355-359.

[46] Rehman A, Park SJ. Comparative study of activation methods to design nitrogen-doped ultra-microporous carbons as efficient contenders for CO_2 capture. Chem. Eng. J. 2018; 352: 539-548.

[47] Rehman A, Park SJ. From chitosan to urea-modified carbons: Tailoring the ultra-microporosity for enhanced CO_2 adsorption. Carbon 2020; 159: 625-637.